Seasonal cycle of the salinity barrier layer revealed in the northeastern Gulf of Guinea

AN Dossa[1,2]*, CY Da-Allada[1,3,4,5] (iD), G Herbert[6] (iD) and B Bourlès[6] (iD)

[1] *International Chair in Mathematical Physics and Applications (ICPMA-UNESCO Chair), University of Abomey-Calavi, Cotonou, Benin*
[2] *Laboratório de Oceanografia Física Estuarina e Costeira, Departamento de Oceanografia, Universidade Federal de Pernambuco (UFPE), Recife-Pernambuco, Brazil*
[3] *Ecole Nationale Supérieure des Travaux Publics (ENSTP)/Université Nationale des Sciences, Technologies, Ingénierie et Mathématiques (UNSTIM), Abomey, Benin*
[4] *Laboratoire d'Hydrologie Marine et Côtière/Institut de Recherches Halieutiques et Océanologiques du Bénin (LHMC/IRHOB), Institut de Recherche pour le Développement (IRD), Cotonou, Benin*
[5] *Institut de Recherche pour le Développement/Laboratoire d'Océanographie Physique et Spatiale (IRD/LOPS), Institut Français de Recherche pour l'Exploitation de la Mer (IFREMER), Centre National de la Recherche Scientifique (CNRS), Université de Brest, Institut Universitaire Européen de la Mer (IUEM), Brest, France*
[6] *Institut de Recherche pour le Développement (IRD), Instrumentation, Moyens Analytiques, Observatoires en Géophysique et Océanographie (IMAGO), Brest, France*
* Corresponding author, e-mail: nath2dossa@gmail.com

The region located in the far northeast of the Gulf of Guinea (NEGG), eastern tropical Atlantic, remains poorly documented due to a lack of available *in situ* ocean data. Heavy rainfall and intense river discharges observed in this region induce a strong salinity stratification that may have a significant impact on the mixed layer depth and on sea surface temperatures, through the so-called barrier-layer effect. By using recent *in situ* data and climatological outputs from a numerical simulation, we reveal the existence of a barrier layer in the NEGG and describe its seasonal occurrence. In the NEGG, the barrier layer limits the mixed layer depth. From January to March, significant values for the barrier-layer thickness are observed mostly due to the horizontal advection of fresh water. From April, vertical mixing along with vertical advection increase the sea surface salinity; hence, the barrier-layer thickness decreases and reaches its minimum in July. During the rest of the year, values for the barrier-layer thickness are again high, mostly under the influence of the Niger River discharge and precipitation, with the highest values recorded in October, when the river discharge and precipitation are at a maximum.

Keywords: mixed layer depth, Niger River discharge, numerical model, oceanography, sea surface salinity, tropical Atlantic, vertical stratification

Introduction

In a classically stratified ocean, the surface layer is virtually homogeneous in temperature, salinity and density. Thus, the layer that is homogeneous in density (also called the mixed layer) is determined by the pycnocline, which is at the same depth as both the halocline and the thermocline. However, in some parts of the ocean, particularly in tropical oceans where strong salinity gradients may be present, a salt stratification may be observed within the isothermal layer. When the halocline and the thermocline no longer coincide, the mixed layer depth is then determined by the halocline. The barrier layer (BL) is a layer that is homogeneous in temperature but stratified in density, and is located between the top of the thermocline and the base of the mixed layer (Godfrey and Lindstrom 1989; Sprintall and Tomczak 1992; de Boyer Montégut et al. 2007; Mignot et al. 2007).

The BL is a physical phenomenon observed in the three tropical oceans. De Boyer Montégut et al. (2007) have shown that the BL is almost permanent in tropical/

subtropical regions, such as the western tropical Atlantic and western Pacific oceans, the Bay of Bengal, the equatorial eastern Indian Ocean and subtropical basins, as well as at high latitudes, such as the Labrador Sea and in parts of the Arctic and Southern oceans. Those authors also showed that the BL appears seasonally in northern subtropical basins, the southern Indian Ocean and the Arabian Sea. Strong precipitation and river runoff have been shown to contribute to BL formation in the Bay of Bengal (Shetye et al. 1996; Varkey et al. 1996; Rao and Sivakuma 2003). Ando and McPhaden (1997) have shown that the main mechanism for BL formation in the western part of the tropical Pacific basin is the strong precipitation observed in that region. The contribution of strong precipitation to BL formation was also confirmed in the western tropical Atlantic basin (Tanguy et al. 2010).

Salinity, through the BL process, can modify heat exchange between the mixed layer and the interior ocean. The BL can reduce cooling through the entrainment of

Published online 24 Jul 2019

surface water. Salt stratification limits the depth of the mixed layer and therefore the amount of solar flux entering the lower ocean layer (Lukas and Lindström 1991; Maes et al. 2002). Thus, positive sea surface temperature (SST) anomalies can persist for a long time-period in the presence of a BL (e.g. Maes et al. 2002). The BL can also limit nutrient transfer into the euphotic zone, with limiting effects on biological productivity (Prasanna Kumar et al. 2004).

The northeastern Gulf of Guinea (NEGG), eastern tropical Atlantic (1°–5° N, 5°–10° E), remains very poorly documented due to a lack of *in situ* ocean data for the region, where strong precipitation and important river runoff (mostly from the Niger River) are observed. According to Dai and Trenberth (2002), the Niger River's discharge (annual mean 7×10^3 m^3 s^{-1}) is the 12th-largest in the world. These freshwater inputs could be expected to lead to a salinity stratification that is likely to generate a BL, similar to that observed off the Amazon River mouth in the western part of the Atlantic basin (Sprintall and Tomczak 1992; Pailler et al. 1999). In the NEGG region, strong precipitation also plays an important role in sea surface salinity (SSS) variability (Berger et al. 2014; Da-Allada et al. 2014a; Camara et al. 2015).

By analysing *in situ* measurements obtained during the French oceanographic cruise EQUALANT, carried out in the boreal summer of 2000, Guiavarc'h (2003) provided evidence of a BL in the NEGG, especially around 3° N, 6° E. More recently, by using the climatology of de Boyer Montégut et al. (2007), Breugem et al. (2008) suggested that the BL does not exist in the NEGG in either the boreal winter (December to February) or boreal summer (June to August). However, very few temperature/salinity data were available for the region (see Figure 2 of de Boyer Montégut et al. 2007). Nonetheless, recent *in situ* data are now available, which, combined with the results of a high-resolution numerical model, allowed a focused study to be conducted in this region. The aim of the present study was thus to verify and confirm the existence of a BL in the NEGG, describe its seasonal cycle, and discuss its potential causes.

Materials and methods

In-situ data
Salinity and temperature data were obtained during the French EQUALANT-2000 and EGEE oceanographic cruises. The EQUALANT-2000 cruise was carried out as a French contribution to the international CLIVAR (CLImate and Ocean – VARiability, Predictability and Change) project (see http://www.clivar.org). Based on three meridional sections carried out in the Gulf of Guinea (along 10° W, 0° E and 6° E), this cruise was implemented on board the RV *Thalassa*, from 25 July to 20 August in 2000 (for details see Bourlès et al. 2002). We used data that were collected at 6° E between 0.33° N and 3.5° N. CTD profiles were carried out every 0°30' in latitude (every 0°20' in the equatorial band between 1° S and 1° N) along all three sections, from 12 to 17 August in 2000. The vertical resolution of the CTD data was 1 m.

In the framework of the program 'Etude de la circulation océanique et du climat dans le Golfe de Guinée' (EGEE) (Bourlès et al. 2007), the French oceanographic component of the African Monsoon Multidisciplinary Analysis (AMMA) program (Redelsperger et al. 2006), six oceanographic surveys were carried out in the Gulf of Guinea from June 2005 to September 2007. We used CTD data that were collected along 6° E every 0°30' of latitude (every 0°20' in the equatorial band between 1° S and 1° N), on 7 and 8 June 2007 during the fifth EGEE cruise (EGEE5) and from 3 to 5 September 2007 during the sixth EGEE cruise (EGEE6). The vertical resolution of the CTD data was 1 m (for details, see Kolodziejczyk et al. 2014).

To investigate the potential causes of the BL, we also used freshwater-input data, namely for precipitation and Niger River runoff. We used precipitation data from ERA-Interim (ERAI) (Dee et al. 2011) and from the Global Precipitation Climatology Project (GPCP) (Adler et al. 2003). Both datasets were available monthly from 1979 to present, with a resolution of 0.75° for ERAI and 2.5° for GPCP. Niger River runoff was determined from altimetry, using the method developed by Papa et al. (2010).

Sea surface salinity (SSS) data were obtained from the SMOS satellite and from the In-Situ Analysis System (ISAS) (Gaillard et al. 2016). The SSS product derived from the SMOS data was L3_DEBIAS_LOCEAN_V3, with improved adjustment of land–sea biases close to the coast (Boutin et al. 2018) and thus suitable for studies close to river plumes. This product was distributed by the Ocean Salinity Expertise Center (CECOS) of the CNES-IFREMER Centre Aval de Traitement des Données SMOS (CATDS) at IFREMER, Plouzané, France. The datasets were 9-day composites at a spatial resolution of 0.25° × 0.25° and were available for the period 2010–2017 (https://www.catds.fr/Products/Available-products-from-CEC-OS/CEC-Locean-L3-Debiased-v3). The ISAS product consisted of climatological gridded fields of temperature and salinity based mainly on autonomous Argo profiling floats and CTD profiles and it was available for the whole period 2002–2016, with a spatial resolution of 0.5° × 0.5° (https://archimer.ifremer.fr/doc/00309/42030/).

The NOAA_OI_SST_V2 dataset, also called the Reynolds product, provided by the NOAA/OAR/ESRL PSD, Boulder, Colorado, USA (https://www.esrl.noaa.gov/psd/), was also used to compare the model seasonal cycle of SST with observations. It was produced on a grid of 0.25° × 0.25°, and was available daily from 1981 to present.

ROMS framework
The numerical simulation results employed were from the Regional Ocean Modeling System (ROMS) framework (Shchepetkin and McWilliams 2005) with a configuration specially adapted to the Gulf of Guinea (Herbert et al. 2016). This model solves the three-dimensional primitive equation of Navier-Stokes following the Boussinesq and hydrostatic approximations. The version of the model used allowed grid refinement (AGRIF code), as follows: a zoom called a 'child' simulation, with a fine mesh (resolution of 1/15°), was nested in a wider domain, called a 'parent' simulation, that was at a lower resolution (1/5°). The wider domain extended from 60° W to 15.3° E, and from 17° S to 8° N, and the finer domain was from 10° W to 14.1° E, and from 17° S to 6° N. The vertical coordinate was discretised into 45 sigma levels, with the vertical *S*-coordinate surface and bottom-stretching parameters set, respectively, to $\theta_s = 6$ and $\theta_b = 0$, to keep sufficient resolution near the surface (Haidvogel and

Beckmann 1999). In the first 150 m, the model had 23 sigma levels. The vertical S-coordinate H_c parameter, which gives the approximate transition depth between the horizontal surface levels and the bottom terrain-following levels, was set to $H_c = 10$ m (Herbert et al. 2016). The Global Earth Bathymetric Chart of the Oceans (GEBCO) 1-resolution dataset was used for the topography (www.gebco.net). The parent simulation was forced at its borders by monthly fields of salinity and temperature, provided by World Ocean Atlas 2009 (WOA09) climatological fields with a spatial resolution of 1° × 1°. Atmospheric forcing on the sea surface (heat, freshwater and wind stress) was provided by Comprehensive Ocean–Atmosphere Data Set (COADS) climatology with a spatial resolution of 1° × 1°. The flows of the major rivers (Amazon, Congo, Niger, Ogooué, Sanaga and Volta rivers) were prescribed monthly from the climatology of Dai and Trenberth (2002). In addition, the model used surface-restoring for salinity.

The simulation was integrated for 15 climatological years, with outputs averaged every 2 days. A statistical equilibrium was reached after 6 years of spin-up. Hence, the model analyses were based on the monthly model outputs averaged from year 7 to year 15.

Criteria for determining the barrier-layer thickness (BLT)

Our computation of the barrier-layer thickness (BLT) was based on the following formula: BLT = ILD – MLD, where ILD is the isothermal layer depth, and MLD is the mixed layer depth. We defined the ILD as the depth where the temperature was 0.5 °C below the SST at the reference depth of 10 m (Monterey and Levitus 1997; Spall et al. 2000; Foltz et al. 2003; de Boyer Montégut et al. 2004; Da-Allada et al. 2015). The MLD was determined using the density (σ) criterion $\Delta\sigma = 0.03$ kg m^{-3} (de Boyer Montégut et al. 2004; Da-Allada et al. 2013); this corresponds to the depth where the density was equal to $\sigma + \Delta\sigma$, where σ is the density at the reference depth of 10 m. The reference depth was chosen at 10 m in order to avoid the strong diurnal cycle that occurs in the first few meters of the ocean (de Boyer Montégut et al. 2004; Da Allada et al. 2015). These criteria for ILD and MLD allowed improved capture of the vertical salinity gradient. Da-Allada et al. (2014a, 2017) used the same criterion for MLD ($\Delta\sigma = 0.03$ kg m^{-3}) to compute the MLD in the Gulf of Guinea.

We also performed sensitivity tests on the MLD and BLT computations. As their values depend on the choice of criteria, we computed different values of MLD and BLT based on different criteria of density, temperature and reference depth. The MLD and BLT monthly errors were estimated as the standard errors of the MLD and BLT computations (Appendix).

Results

Model validation

Mean states of sea surface salinity (SSS) and temperature (SST)

The spatial distributions of the annual mean SSS from the ROMS model and from the SMOS and ISAS products are shown in Figure 1. The model and both the SMOS and ISAS products showed very similar patterns, with high SSS (~36)
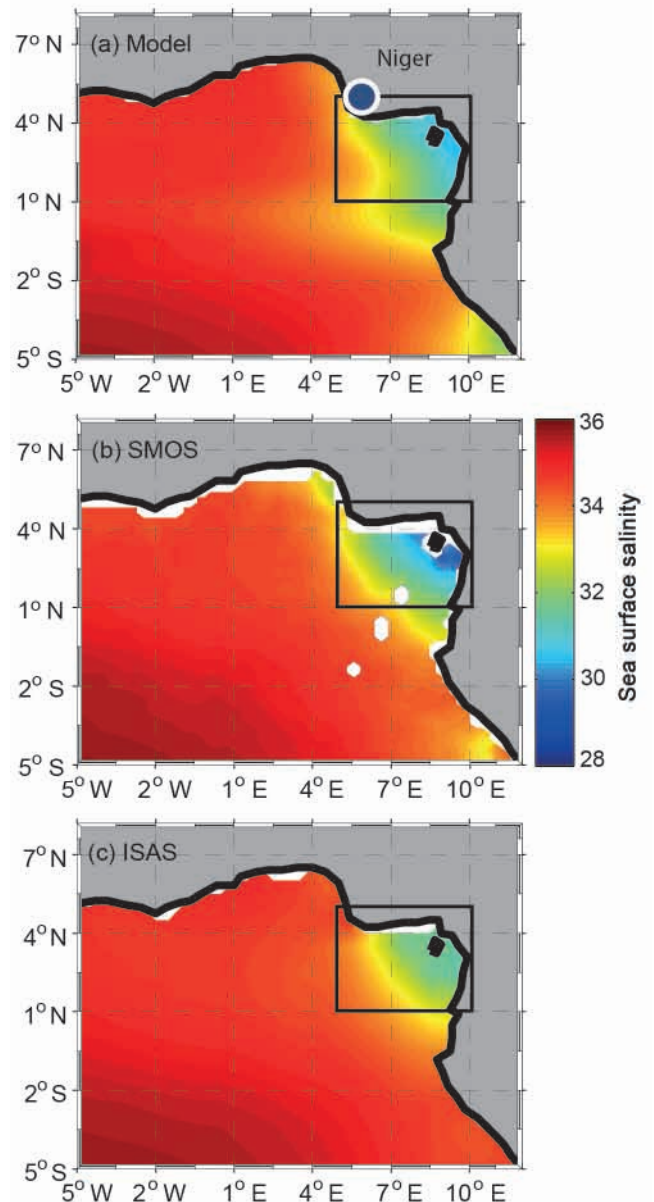

Figure 1: Annual mean sea surface salinity from (a) ROMS model, (b) SMOS product, and (c) ISAS product in the Gulf of Guinea, West Africa. Boxes indicate the focal area of study (defined here as the northeastern Gulf of Guinea [NEGG]). The position of the Niger River mouth is indicated in (a)

found in the southwestern region, and low SSS (~31) found in the northeastern region of the Gulf of Guinea, near the African coast. This region is under the influence of the Niger River discharge and high precipitation, enhanced by the presence of Mount Cameroon. The model exhibited another region with a low SSS value in the vicinity of 5° S, close to the coast between 10° E and 12° E, attributable to the Congo River discharge. This region of low SSS was also detected by the SMOS product. In contrast, the ISAS product did not exhibit such low SSS values in this region. Also, the SMOS product captured the low SSS values in the northeastern

region better than the ISAS. This difference may be explained by the low number of *in situ* data available to build the ISAS product (Figure 2 in Gaillard et al. 2016).

The model reproduced the spatial distribution of the observed SST reasonably well (Figure 2). Both the model and the observations exhibited an SST maximum (>27 °C) north of the equator, from 5° W to the African coast. However, the model seemed to slightly underestimate the SST, as was visible from 5° W to 2° W along the equator. South of the equator, a weaker SST (<27 °C) was recorded from 5° W to 12° E, both by the model and from observations.

These comparisons showed that the ROMS model produced a satisfactory simulation of spatial distributions of SSS and SST.

Seasonal variability in SSS and SST

Seasonal cycles of SSS and SST in the NEGG area (1°–5° N, 5°–10° E), deduced from the ROMS model and from the observations (SMOS and ISAS for SSS, and Reynolds for SST), are shown in Figure 3. Both SSS and SST exhibited seasonal variation in the NEGG. The SSS seasonality simulated by the model presented maximum values between July and September and minimum values between January and February. The model output represented an underestimate compared with the ISAS observations from December to September, with a bias of 2.4 in February, but an overestimate from September to November, with a bias of 0.2 in October. When compared with the SMOS observations, the model underestimated SSS from January to July (with a bias of 0.6 in April) and overestimated SSS during the rest of the year (with a bias of 1.8 in November). The lag of ~1 month between the model output and the maxima and minima in the observations might be due to uncertainties in freshwater forcing. The model reproduced the seasonality of observed SST reasonably well throughout the year. Maximum SST values (>27.5 °C) were found from January to April, and minimum values (<27.4 °C) from May to December. However, the model presented a cold bias (of −0.7 °C in April, and −0.9 °C in August) throughout the year.

Despite the biases, which were relatively small, the model reproduced the seasonality in SSS and SST adequately and was thus considered to be appropriate for the current study.

Vertical distributions in salinity and temperature

EQUALANT-2000 observations and the ROMS model output at 6° E in August — The vertical distribution of salinity in August is shown from the EQUALANT-2000
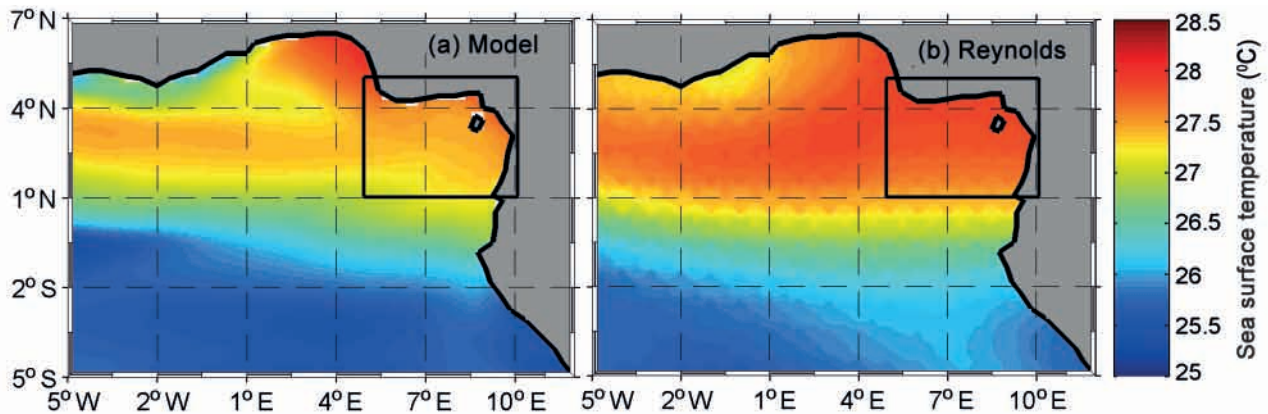

Figure 2: Annual mean sea surface temperature (SST) from (a) the ROMS model and (b) the Reynolds product. Boxes indicate the focal area of study (northeastern Gulf of Guinea, West Africa)
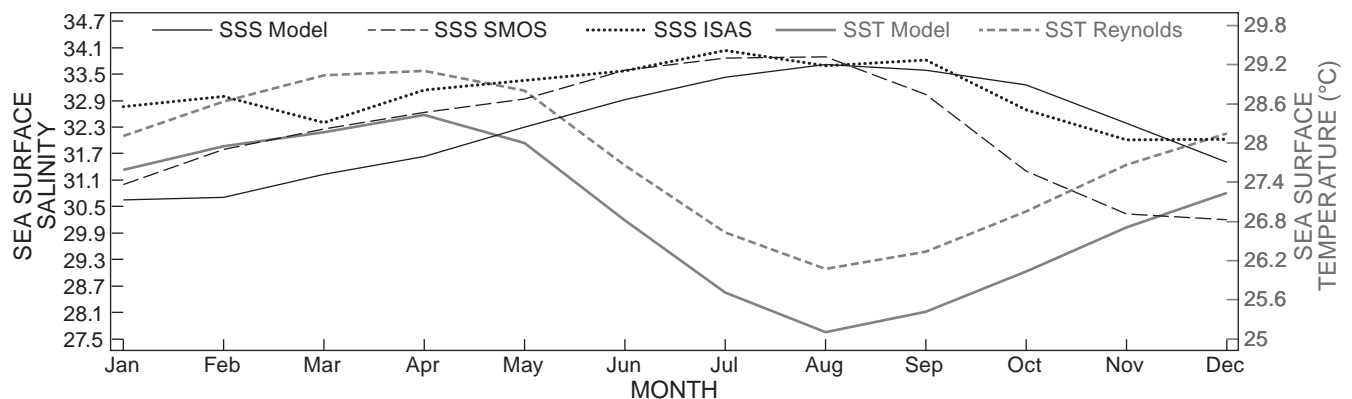

Figure 3: Seasonality of sea surface salinity (SSS) and sea surface temperature (SST) for the SMOS and Reynolds products and for the ISAS product and the ROMS model, in the northeastern Gulf of Guinea, West Africa

cruise (Figure 4a) and from the model (Figure 4b) along 6° E from 0° N to 3.5° N. The EQUALANT-2000 salinity values were obtained from 12 to 17 August 2000, whereas the model salinity was a monthly average for August. The EQUALANT-2000 data exhibited a fresh layer between 0.33° N and 2.5° N, extending from the surface down to a depth of 30 m, with values between 33.5 and 34.5. This fresh layer was also simulated by the model. At 3.5° N, another fresh layer was observed at the surface, with a thickness of 20 m, both in the model output and in the EQUALANT-2000 data, although the *in situ* data revealed saltier conditions (~34.5) than the simulated data (~34). Below 40 m, salinity values were above 35.5 in both the model output and the EQUALANT-2000 data.

A warm surface layer with a thickness of approximately 35 m was present in both the EQUALANT-2000 data and in the model output, with SST values higher than 25 °C, as illustrated on the vertical sections for temperature (Figure 5). The thermocline was apparent at a depth of ~35 m in both the EQUALANT-2000 data and the model output, and the temperature decreased with depths below 40 m.

EGEE5 observations and model output at 6° E in June — In June, both the EGEE5 data (Figure 6a) and the model output (Figure 6b) showed a fresh surface layer with salinity of ~33. Below 40 m depth, the salinity increased strongly and exhibited maximum values of up to 36 at 50–60 m depth. The temperature profiles from the EGEE5 observations (Figure 7a) and the model output (Figure 7b) both exhibited a warm surface layer (>26 °C). Below this layer, the model simulated well the temperature decrease with depth, from 22 °C at ~40 m to 14 °C at ~120 m.

Hence, the ROMS model adequately reproduced the vertical distribution of salinity and temperature in June along 6° E from 0.5° N to 2.5° N.

EGEE6 observations and model output at 6° E in September — Data from EGEE6 were available from 3 to 5 September 2007. The salinity vertical section (Figure 8a) showed an important fresh layer north of 2.5° N from the surface down to a depth of 20 m, with values as low as 32. This local freshwater layer was also present in the model output (Figure 8b). However, the salinity values from the model were higher (~33.5). Also, both the model output and the observations suggested a weak decrease in salinity above ~30 m between 0° N and 1° N.

Both the EGEE6 observations and the model output exhibited a warm surface layer (>25 °C) north of 1° N, extending down to the thermocline (Figure 9). The model simulated a more diffuse and shallower thermocline (i.e. at ~50 m depth) than was reflected in the observations (at ~60 m depth). However, both model and observations exhibited the same thermocline shape, deeper at ~2° N and shallower close to the coast in the north.

Hence, the model adequately reproduced the spatial (horizontal and vertical) distribution of SSS and SST in September along 6° E, and thus its use was considered appropriate to verify the existence of a BL and to analyse its spatial and temporal variations.

Evidence of a barrier layer in the northeastern Gulf of Guinea
Below, we compare the output of the ROMS model to observations that were available in August and September only.
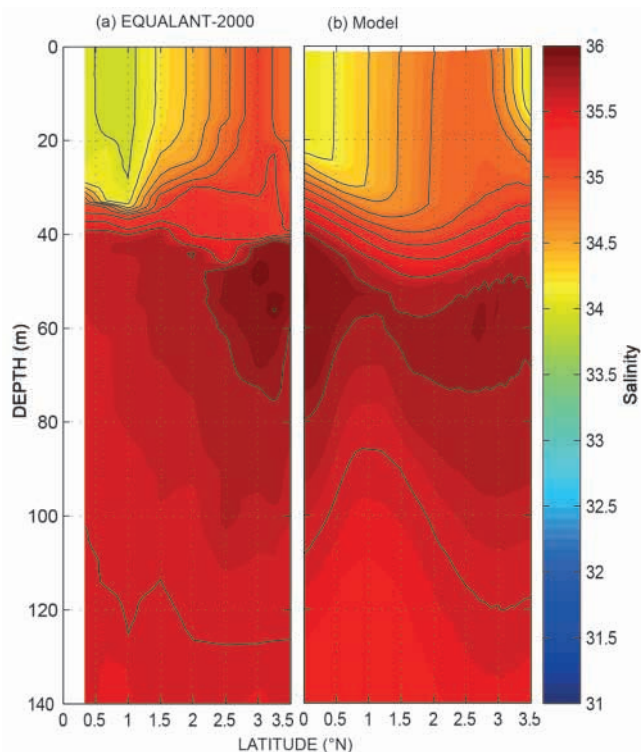

Figure 4: Vertical sections of salinity in August, from (a) the EQUALANT-2000 cruise and (b) the ROMS model, along 6° E between 0° N and 3°50′ N, from the surface to a depth of 140 m
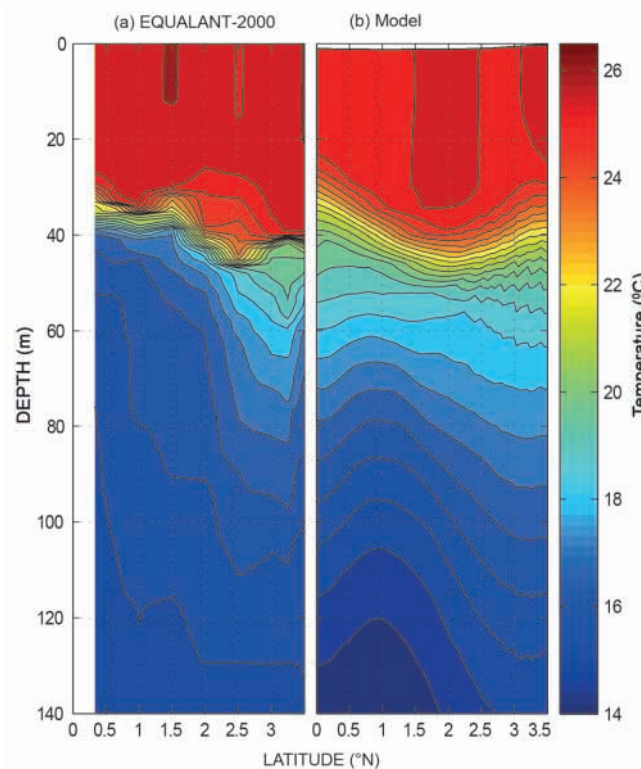

Figure 5: Vertical sections of temperature in August, from (a) the EQUALANT-2000 cruise and (b) the ROMS model, along 6° E between 0° N and 3.5° N, from the surface to a depth of 140 m
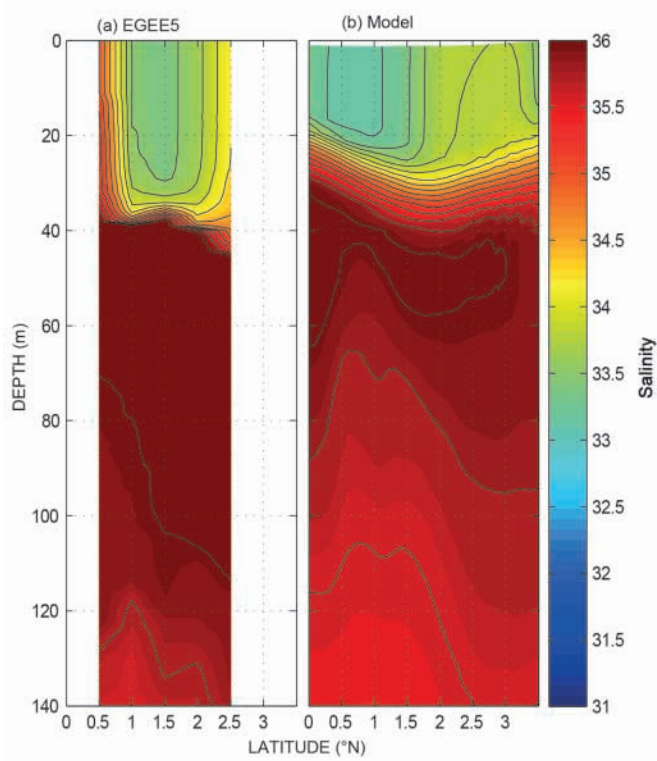
Figure 6: Vertical sections of salinity in June, from (a) the EGEE5 cruise and (b) the ROMS model, along 6° E between 0° N and 3°50 N, from the surface to a depth of 140 m
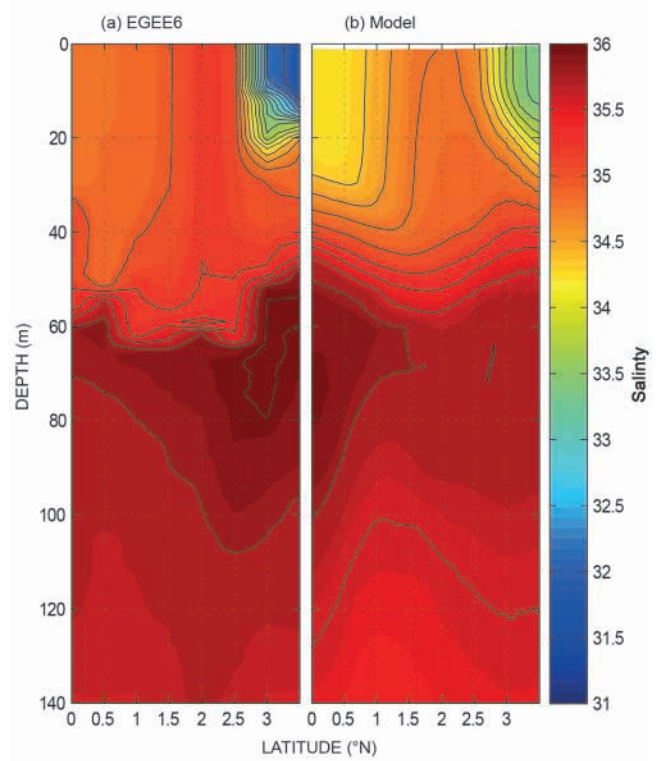

Figure 8: Vertical sections of salinity in September, from (a) the EGEE6 cruise and (b) the ROMS model, along 6° E between 0° N and 3.5° N, from the surface to a depth of 140 m
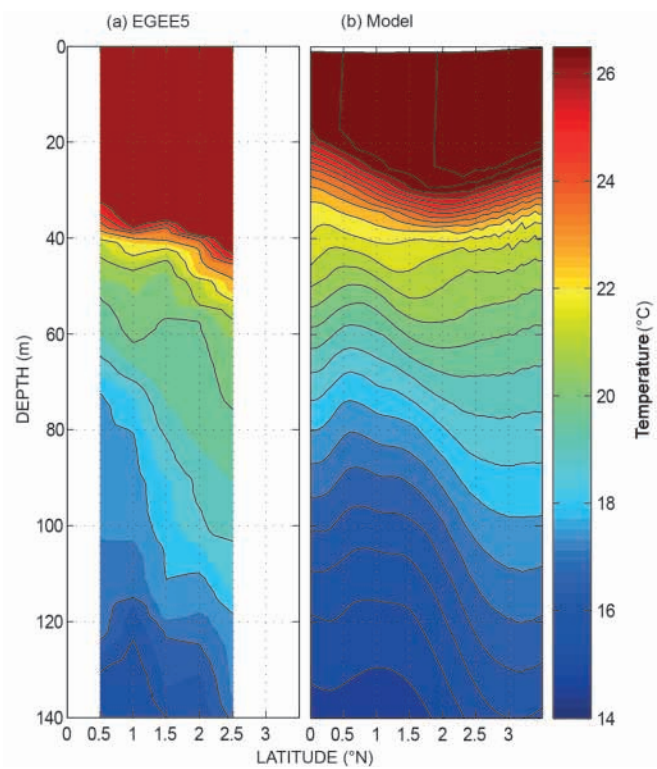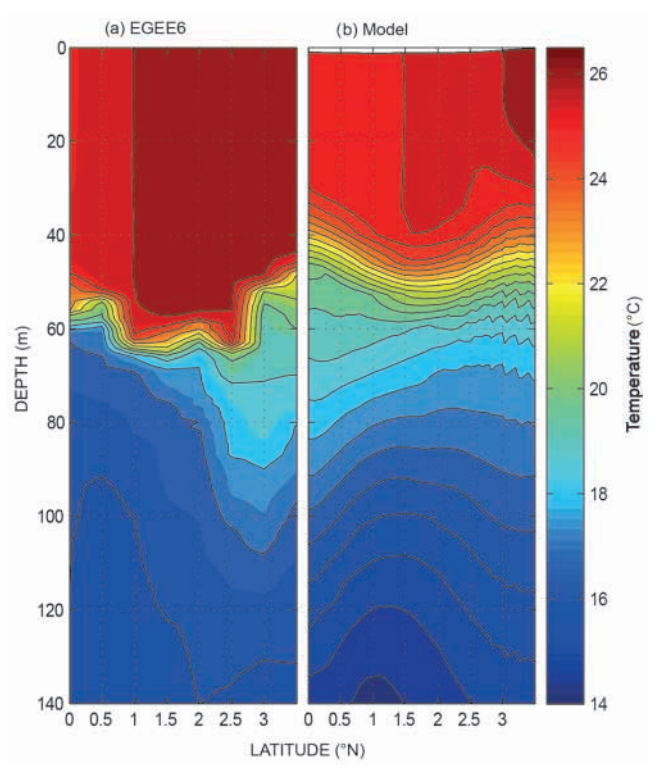

Figure 7: Vertical sections of ocean temperature in June, from (a) the EGEE5 cruise and (b) the ROMS model, along 6° E between 0° N and 3.5° N, from the surface to a depth of 140 m

Figure 9: Vertical sections of ocean temperature in September, from (a) the EGEE6 cruise and (b) the ROMS model, along 6° E between 0° N and 3.5° N, from the surface to a depth of 140 m

August profiles
Vertical profiles of temperature, salinity and density are shown from EQUALANT-2000 observations (Figure 10a), the model output (Figure 10b) and from ISAS (Figure 10c). The *in situ* EQUALANT-2000 data were available for 12 August 2000, and the model and ISAS profiles for the month of August across multiple years.

The *in situ* profiles of EQUALANT-2000 exhibited a surface layer of 20-m thickness, homogeneous in salinity, temperature and density (Figure 10a). In the model, this homogeneous surface layer exhibited a thickness of 12 m (Figure 10b). The *in situ* observations showed two clear salinity vertical gradients, at 20 m and 40 m (Figure 10a). At 20 m depth, the observed temperature underwent a slight change from 26° to 25.5 °C. In the same layer, the density profile also presented clear gradients, at the same depths as the salinity gradients. According to the definition of BL (see above), it is apparent that the observations revealed a BL of 20-m thickness, at between 20 and 40 m depth (Figure 10a). In the model, the salinity profile also showed vertical gradients around 15 and 30 m, although less marked than in the EQUALANT-2000 observations. However, these gradients were also apparent in the temperature and density profiles, clearly indicating the presence of a BL of 15-m thickness between 15 and 30 m (Figure 10b). In addition, the monthly mean of the BLT obtained from the model was compared with that obtained from the ISAS at 3.25° N and 6° E in August. ISAS exhibited a BLT of 21 m (Figure 10c), a difference of 6 m when compared with the model.

September profiles
An equivalent comparison as for August, above, was made for September, but with observations from EGEE6 recorded on 3 September 2007. The EGEE6 data provided evidence of a BL of ~32-m thickness (Figure 11a). The monthly average data from the model for September suggested a BL of 14-m thickness (Figure 11b). The important BLT value recorded from the EGEE6 data might be associated with the desalinisation that occurred during the same month around the same position (Figure 8a).

Furthermore, we compared the monthly mean of the BLT obtained from the model with that from the ISAS data at the position 3.5° N, 6° E in September. The BLT from the ISAS data was 10-m thicker than that simulated by the model (Figure 11c). The difference might be linked to the spatial distribution of the BLT in the model, as it might be extended westward during this period of the year.

Mean state and seasonal cycle of the BLT in the NEGG
Here we describe the BLT mean state and its seasonal spatial distribution as computed from the model monthly average output, with a particular focus on the NEGG region.

Annual mean of the BLT
The annual mean of the BLT computed from the model output and the annual mean of the precipitation are presented in Figure 12. The presence of a substantial BLT (>10 m) was evident in the area 1–6° N, 3–10° E, with thicknesses in the NEGG of up to 17 m at around 2° N, 7° E. In the same region the mean precipitation from the ERAI data was at a maximum, with values of up to
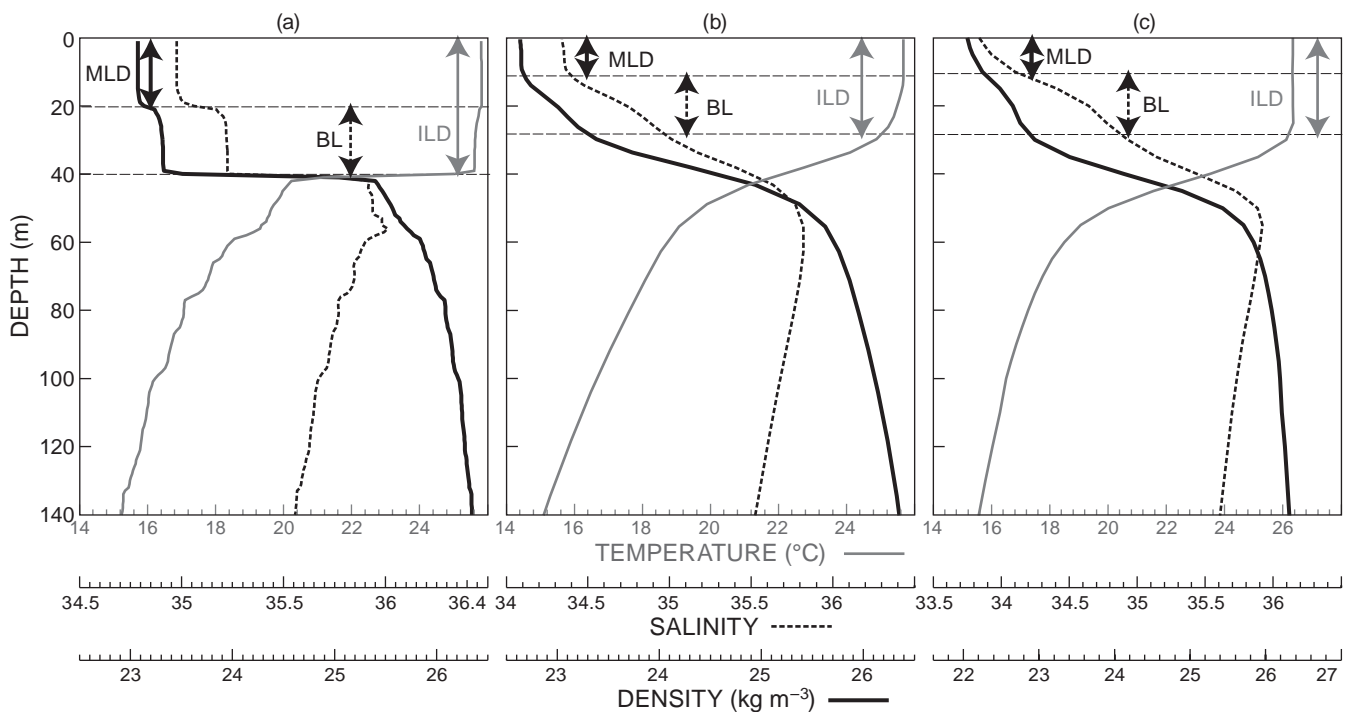

Figure 10: Profiles of ocean temperature, salinity and density at the location 3.25° N, 6° E, as obtained from: (a) observations from the EQUALANT-2000 cruise, recorded on 12 August 2000; (b) the ROMS model; and (c) data from the ISAS product, recorded in August. BL = barrier layer; ILD = isothermal layer depth; MLD = mixed layer depth

10 mm day⁻¹ (Figure 12b). In its mean state, the region where the BL was present corresponded to the region where low SSS values (see Figure 1) and significant precipitation were observed. Just as low values of SSS are related to precipitation and river runoff, so too are BLT values induced by precipitation and river runoff in this region.

Monthly variation in distribution and thickness of the BLT
To analyse the extent and seasonal variations of the BL in the Gulf of Guinea, monthly maps of the BLT, from January to December, over the region 6° N, 5° W–5° S, 12° E, were computed from the ROMS simulation output

(Figure 13). The extent of the BL in the Gulf of Guinea showed considerable variation. From January to April the BL extended over a large part of the Gulf of Guinea, and the highest values of the BLT (>20 m) were observed in the NEGG in February and March. The extent of the BL decreased from May until July and remained in the most northeastern region close to the coast. From August the extent of the BL increased again with the thickness at >22 m, until October when a robust BL extended over the whole NEGG, from around 5° W to 10° E at ~1° N. In October the BL was also observed along the coast south of the equator, with thickness values of ~10 m. In November
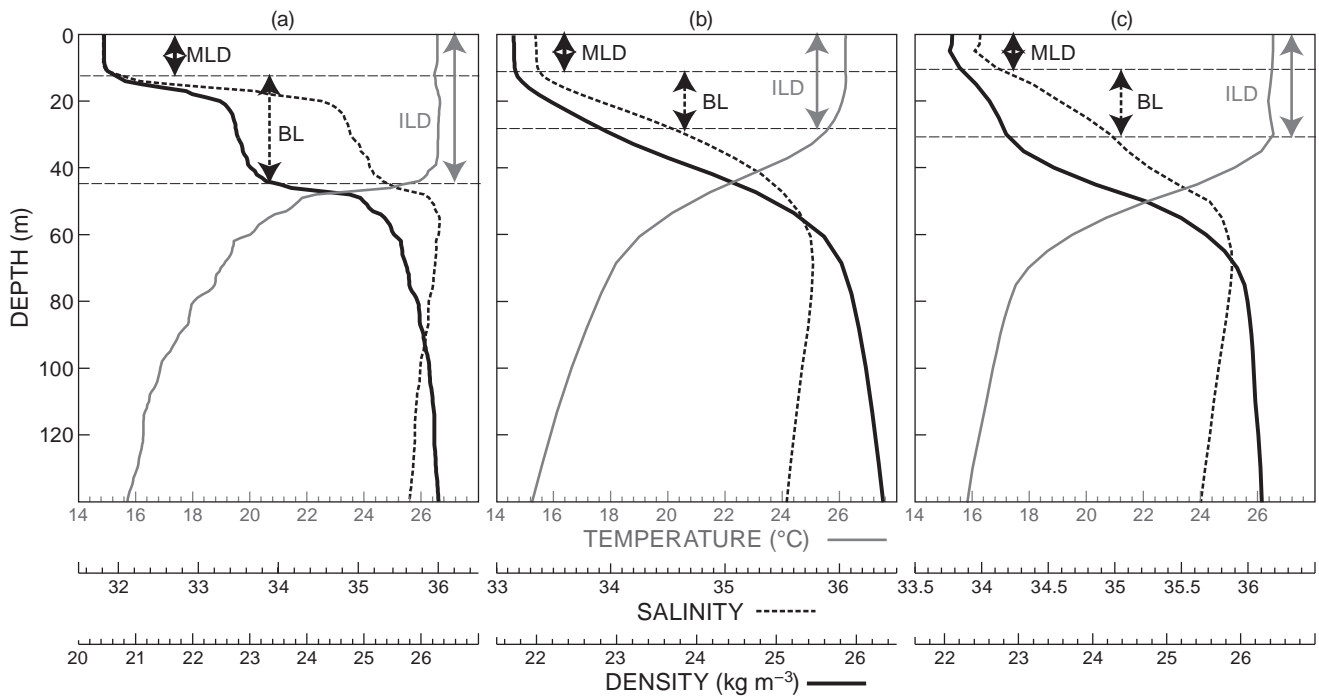

Figure 11: Profiles of ocean temperature, salinity and density at the location 3.5° N, 6° E, as obtained from: (a) observations from the EGEE6 cruise, recorded on 3 September 2007; (b) the ROMS model; and (c) data from the ISAS product, recorded in September. BL = barrier layer; ILD = isothermal layer depth; MLD = mixed layer depth
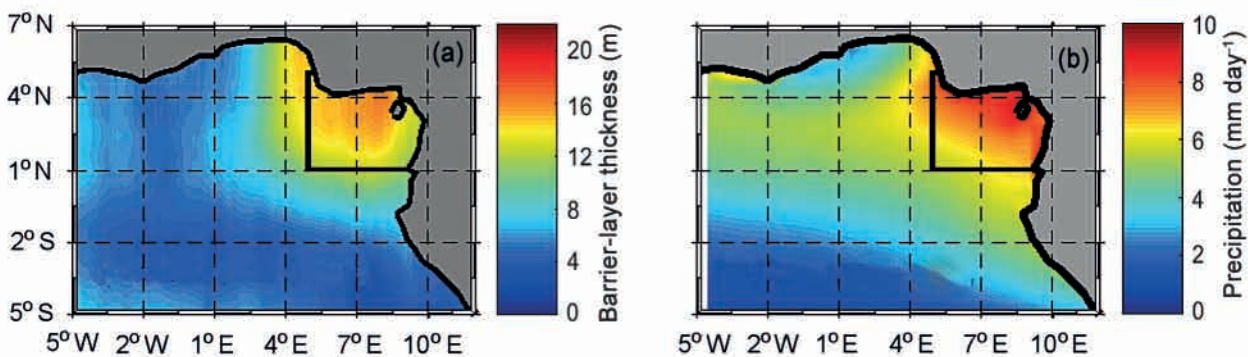

Figure 12: (a) Annual mean of the barrier-layer thickness in the northeastern Gulf of Guinea, West Africa, computed from the ROMS simulation, and (b) annual mean of precipitation computed from the ERA-Interim product. Boxes indicate the focal area of the study

and December the BL still extended over a large part of the NEGG but with decreasing thickness values.

Seasonal cycle of the barrier layer and its impact on the mixed layer depth

Seasonal cycles of the SSS, the MLD (with estimated error) and the BLT (with estimated error) obtained from the ROMS model are shown in Figure 14. SSS, as previously described (Figure 3), exhibited distinct seasonality, with maximum values in August/September (>33.3) and minimum values in January/February (<31). The seasonal occurrence of the BL in the NEGG was analysed in terms of its thickness (i.e. the BLT). The BLT was greater than 10 m from January to March, then decreased until August,

with a minimum in May, June and July (<6 m). The BLT then increased to a maximum of 18 m in October, before decreasing again to 10 m in December. Hence there were two main seasons with regard to the BL: the first from September to March, with relatively high BLT values, and the second from April to August, when the BLT was weaker. The weakest values of the MLD were associated with high values of the BLT, and conversely high values of the MLD were associated with the lowest BLT values. This suggests that the BL affects the MLD by limiting its depth. The inverse relationships between SST and SSS, along the sections at 6° E carried out during the EQUALANT-2000 and EGEE6 cruises, might indicate a potential impact of the BL on SST.
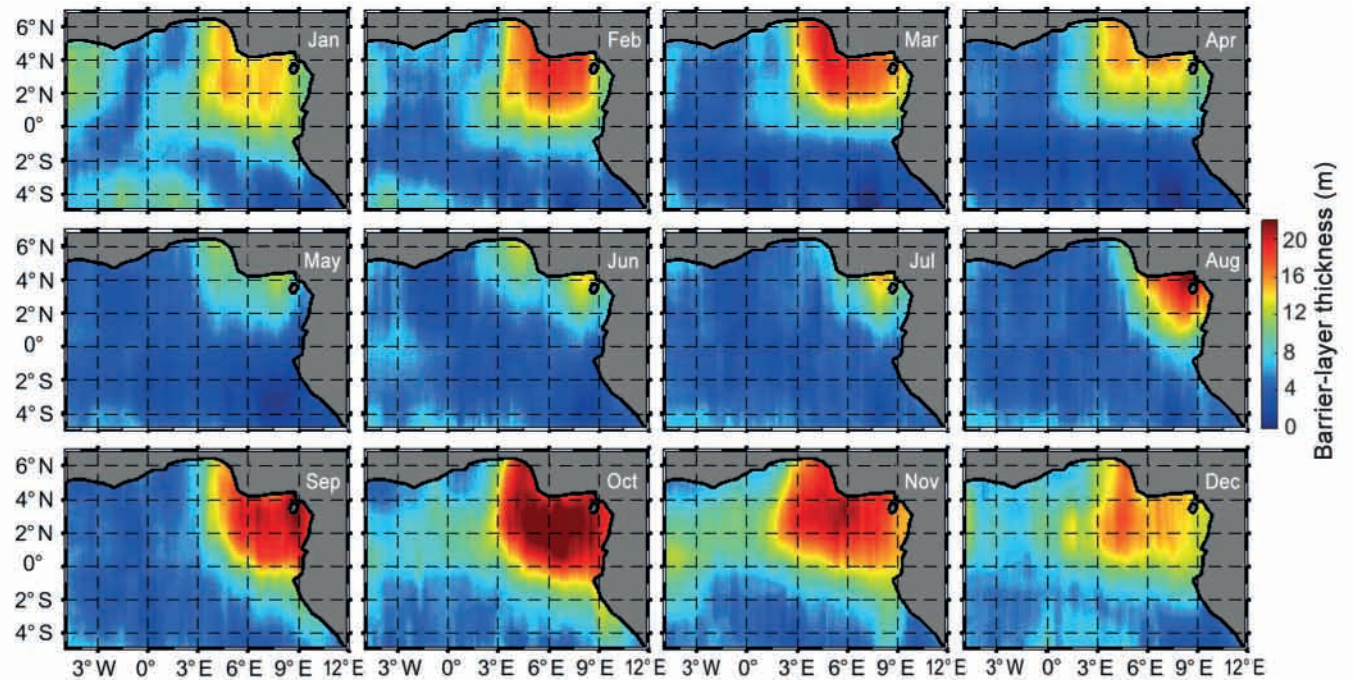

Figure 13: Monthly maps of the barrier-layer thickness in the Gulf of Guinea, West Africa, as computed from the ROMS simulation
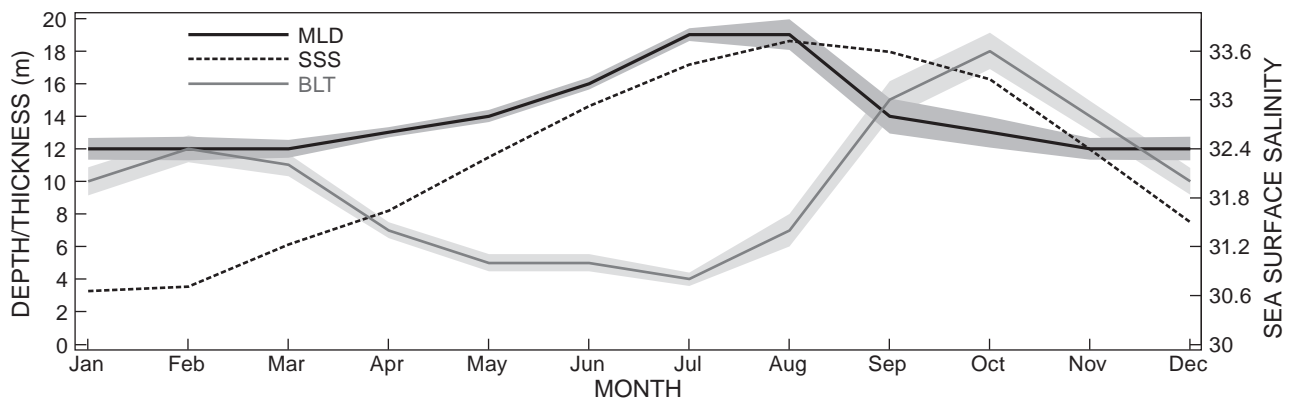

Figure 14: Seasonal cycles in the northeastern Gulf of Guinea and as inferred from the ROMS simulation of sea surface salinity (SSS), barrier-layer thickness (BLT), and mixed layer depth (MLD); shaded areas indicate standard deviations estimated by means of sensitivity tests (see Appendix)

Discussion

To our knowledge, and probably due to the lack of *in situ* data for the region, previous studies have not pointed out the presence and seasonal occurrence of any BL in the NEGG. In this study, we have revealed the existence of the BL and described its seasonal cycle in the NEGG by using a ROMS model and available *in situ* observations. Although Guiavarc'h (2003), using *in situ* data, had suggested the existence of the BL, its formation had not been well documented due to insufficient data. We computed the BLT based on temperature and density criteria, and our computation was performed with a sensitivity test using the criteria 0.5 °C for the ILD and 0.03 kg m^{-3} for the MLD. These criteria had been shown in previous studies to be most suitable for capturing the vertical salinity gradient (Tanguy et al. 2010; Da Allada et al. 2014a, 2017).

Using a ROMS simulation, we have shown that the annual mean BL is present in a large part of the Gulf of Guinea, extending from 5° S to 7° N and from 5° W to 12° E. In particular, the northeastern area (1°–6° N, 3°–10° E), bordered by the coast of West Africa, exhibits a robust BL pattern with maximal BLT values. These large BLT values in the NEGG, where the BL is observed throughout the year, are induced mainly by the contributions of river discharge and precipitation. Hence, we focused on the NEGG region.

We have also shown that the BL in the NEGG exhibits a seasonal pattern, with the extent of the BL being at a maximum during February and October and at a minimum in July. The BL seasonally affects the MLD by limiting its depth, and the BLT and the MLD vary in an opposite phase. Also, in August/September, when the BL is confined to the NEGG, the SST is at a maximum and is associated with minimum values of SSS.

Figure 15 shows seasonal cycles of the BLT in the NEGG, the Niger River discharge and precipitation from two products, ERAI and GPCP, which exhibited similar cycles. Here, we diagnose the relative contributions of the Niger River discharge and precipitation to seasonality in the BL. Precipitation was highest in October (~10.5 mm day^{-1} from ERAI, and 9 mm day^{-1} from GPCP), and lowest in January/February. This region is under the influence of the Inter-Tropical Convergence Zone (ITCZ) which affects the seasonal variability of rain in the NEGG. The Niger River discharge was low from January to July before increasing to a maximum in October and then decreasing again. The coincident low precipitation and Niger River discharge from January to March indicate that these cannot be responsible for the high BLT levels recorded during these particular months; hence, it appears that other processes influence the BL during this period. Da-Allada et al. (2014b) found that a seasonal decrease in the salinity of the mixed layer in the NEGG was a consequence of both freshwater flux (precipitation plus runoff) and horizontal advection. Therefore, the horizontal advection of fresh water might be the mechanism inducing high BLT values at the beginning of the year. The BLT then decreased from March to a minimum of 4 m in July, which is a period during which high precipitation was recorded (maximum in May and June) before a decrease, but the Niger River discharge remained low. A recorded increase in SSS from May to August in the Bight of Biafra is due to vertical advection and vertical mixing (Berger et al. 2014; Da-Allada et al. 2014b). Consequently, these vertical processes contribute to a decrease in the BLT by increasing salinity of the mixed layer. The BLT in the NEGG increased from August, to a maximum of 18 m in October, and then decreased to 10 m in December, during which period precipitation and the Niger River discharge followed a similar trend. Given the coincident maxima in October in the Niger River discharge, precipitation and the BLT, it can be deduced that the strong BL from August to December is directly induced by precipitation and the Niger River runoff.

It appears that the mechanism that induces the BL is the presence of low-salinity surface water in the region. A similar result was found by Pailler et al. (1999) in the western tropical Atlantic. Using *in situ* and high-resolution
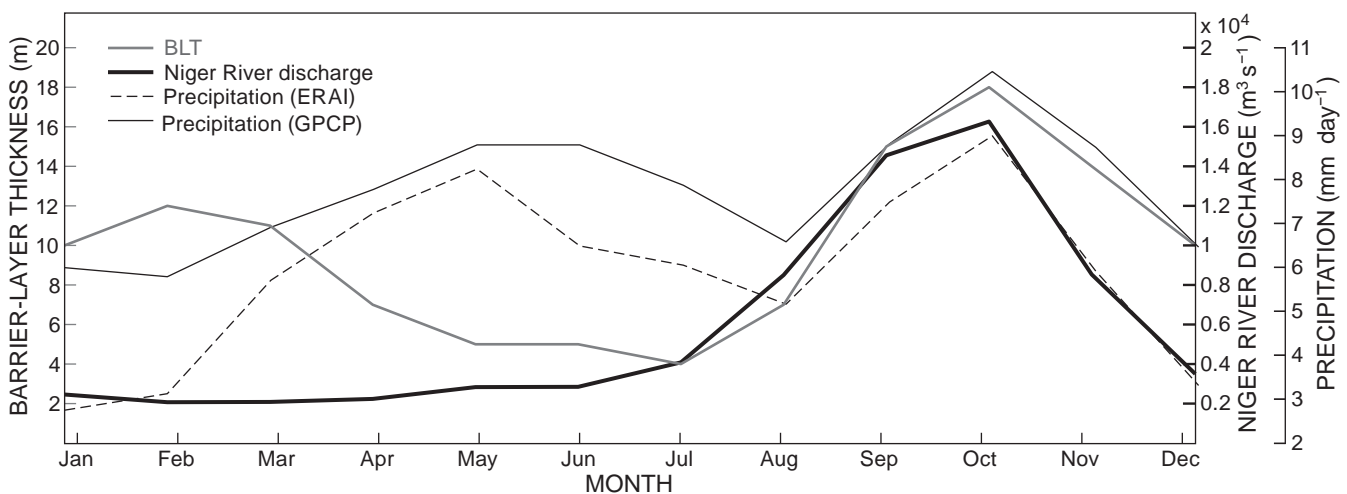

Figure 15: Seasonal cycles of the barrier-layer thickness (BLT) in the northeastern Gulf of Guinea computed from the ROMS simulation, values of Niger River discharge and precipitation, from the ERA-Interim product (ERAI) and the Global Precipitation Climatology Project (GPCP)

CTD data, they suggested that fresh water from the Amazon River may induce a strong halocline that generates a BL. Also, Cronin and McPhaden (2002) noted that a BL can be formed through rainfall which, in the absence of strong mixing and surface heating, can induce BL formation between the fresh lens and the top of the isothermal layer.

Ocean currents might cause a BL to be advected horizontally from its region of formation (Cronin and McPhaden 2002). In the northern Gulf of Guinea, two major currents are present: the Guinea Current and the South Equatorial Current (Hisard 1975; Hisard and Merle 1979). The eastward-flowing Guinea Current is observed between the coast and the northern branch of the South Equatorial Current, between 2° N and 4° N, depending on season (Donguy and Privé 1964). Variations of these currents might be one of the mechanisms responsible for the seasonal extension of the BL into the Gulf of Guinea.

In this study, in agreement with the studies of Guiavarc'h (2003) but contrary to Breugem et al. (2008), we observed a BL in the NEGG with a well-marked seasonal cycle. The BL could not be observed by previous studies due to a lack of *in situ* surface and subsurface data for this region. We combined recently available *in situ* data for the NEGG with climatologic simulation outputs. The ROMS model used surface-restoring for salinity, and it is noted that this could affect the simulated salinity results (e.g. Large et al. 1997; Behrens et al. 2013). Although the model reproduced the vertical salinity distribution well, it would be interesting to revisit our results by using a numerical model without surface-restoring.

ORCID

Bernard Bourles https://orcid.org/0000-0001-6515-4519
Casimir Da-Allada https://orcid.org/0000-0002-9147-445X
Gaëlle Herbert https://orcid.org/0000-0001-8911-9697

References

Adler RF, Huffman GJ, Chang A, Ferraro R, Xie P, Janowiak J et al. 2003. The Version-2 Global Precipitation Climatology Project (GPCP) monthly precipitation analysis (1979–present). *Journal of Hydrometeorology* 4: 1147–1167.

Ando K, McPhaden MJ. 1997. Variability of surface layer hydrography in the tropical Pacific Ocean. *Journal of Geophysical Research* 102(C10): 23063–23078.

Behrens E, Biastoch A, Böning CW. 2013. Spurious AMOC trends in global ocean sea-ice models related to subarctic freshwater forcing. *Ocean Modelling* 69: 39–49.

Berger H, Tréguier A, Perenne N, Talandier C. 2014. Dynamical contribution to sea surface salinity variations in the eastern Gulf of Guinea based on numerical modeling. *Climate Dynamics* 43: 3105–3122.

Bourlès B, D'Orgeville M, Eldin G, Chuchla R, Gouriou Y, du Penhoat Y, Arnault S. 2002. On the thermocline and subthermocline eastward currents evolution in the Eastern Equatorial Atlantic. *Geophysical Research Letters* 29: 32-1–32-4.

Bourlès B, Brandt P, Caniaux G, Dengler M, Gouriou Y, Key E et al. 2007. African Monsoon Multidisciplinary Analysis (AMMA): special measurements in the tropical Atlantic. *CLIVAR Exchange* No. 41 (vol. 12). Qingdao, China: Climate Variability and Predictability Programme. pp 7–9.

Boutin J, Vergely JL, Marchand S, D'Amico F, Hasson A, Kolodziejczyk N et al. 2018. New SMOS sea surface salinity with reduced systematic errors and improved variability. *Remote Sensing of Environment* 214: 115–134.

Breugem W-P, Chang P, Jang CJ, Mignot J, Hazeleger W. 2008. Barrier layers and tropical Atlantic SST biases in coupled GCMs. *Tellus Series A* 60: 885–897.

Camara I, Kolodziejczyk N, Mignot J, Lazar A, Gaye AT 2015. On the seasonal variations of salinity of the tropical Atlantic mixed layer. *Journal of Geophysical Research: Oceans* 120: 4441–4462.

Cronin MF, McPhaden MJ. 2002. Barrier layer formation during westerly wind bursts. *Journal of Geophysical Research: Oceans* 107(C12): SRF 21-1–SRF 21-12.

Da-Allada CY, Alory G, du Penhoat Y, Kestenare E, Durand F, Hounkonnou NM. 2013. Seasonal mixed-layer salinity balance in the Tropical Atlantic Ocean: mean state and seasonal cycle. *Journal of Geophysical Research: Oceans* 118: 332–345.

Da-Allada CY, Alory G, du Penhoat Y, Jouanno J, Hounkonnou NM, Kestanare E. 2014a. Causes for the recent increase in sea surface salinity in the north-eastern Gulf of Guinea. *African Journal of Marine Science* 36: 197–205.

Da-Allada CY, du Penhoat Y, Jouanno J, Alory G, Hounkonnou NM. 2014b. Modeled mixed-layer salinity balance in the Gulf of Guinea: seasonal and interannual variability. *Ocean Dynamics* 64: 1783–1802.

Da-Allada CY, Gaillard F, Kolodziejczyk N. 2015. Mixed-layer salinity budget in the tropical Indian Ocean: seasonal cycle based only from observations. *Ocean Dynamics* 65: 845–857.

Da-Allada CY, Jouanno J, Gaillard F, Kolodziejczyk N, Maes C, Reul N, Bourlès B. 2017. Importance of the Equatorial Undercurrent on the sea surface salinity in the eastern equatorial Atlantic in boreal spring. *Journal of Geophysical Research: Oceans* 122: 521–538.

Dai A, Trenberth K. 2002. Estimates of freshwater discharge from continents: latitudinal and seasonal variations. *Journal of Hydrometeorology* 3: 660–687.

de Boyer Montégut CB, Madec G, Fischer AS, Lazar A, Ludicone D. 2004. Mixed layer depth over the global ocean: an examination of profile data and a profile-based climatology. *Journal of Geophysical Research* 109: C12003.

de Boyer Montégut CB, Mignot J, Lazar A, Cravatte S. 2007. Control of salinity on the mixed layer depth in the world ocean: 1. General description. *Journal of Geophysical Research* 112: C06011.

Dee DP, Uppala SM, Simmons AJ, Berrisford P, Poli P, Kobayashi S et al. 2011. The ERA-Interim reanalysis: configuration and performance of the data assimilation system. *Quarterly Journal of the Royal Meteorological Society* 137: 553–597.

Donguy JR, Privé M. 1964. Les conditions de l'Atlantique entre Abidjan et l'équateur – 2e partie. Variations hydrauliques annuelles entre Abidjan et l'Equateur. *Cahiers Océanographiques* 16: 393-398.

Foltz GR, Grodsky SA, Carton JA. 2003. Seasonal mixed layer heat budget of the tropical Atlantic Ocean. *Journal of Geophysical Research* 108: 3146.

Gaillard F, Reynaud T, Thierry V, Kolodziejczyk N, von Schuckmann K. 2016. *In situ* based reanalysis of the global ocean temperature and salinity with ISAS: variability of the heat content and steric height. *Journal of Climate* 29: 1305–1323.

Godfrey JS, Lindstrom EJ. 1989. The heat budget of the equatorial western Pacific surface mixed layer. *Journal of Geophysical Research* 94: 8007–8017.

Guiavarc'h C. 2003. Analyse de la salinité dans les couches supérieures du Golfe de Guinée. Rapport de stage de DEA Océanologie, Météorologie et Environnement. Brest, France: Université de Bretagne Occidentale.

Haidvogel DB, Beckmann A. 1999. Numerical ocean circulation modeling. London: Imperial College Press.

Herbert G, Bourlès B, Penven P, Grelet J. 2016. New insight on the upper layer circulation north of Gulf of Guinea. *Journal of Geophysical Research: Oceans* 121: 6793–6815.

Hisard P. 1975. La circulation superficielle dans la partie occidentale du Golfe de Guinée. *Documents Scientifiques* No. 6. Abidjan: Centre de Recherches Océanographiques. pp 41–57.

Hisard P, Merle J. 1979. Onset of summer surface cooling in the Gulf of Guinea during GATE. *Deep-Sea Research* 26 (suppl.): 325–341.

Kolodziejczyk N, Marin F, Bourlès B, Gouriou Y, Berger H. 2014. Seasonal variability of the Equatorial Undercurrent termination and associated salinity maximum in the Gulf of Guinea. *Climate Dynamics* 43: 3025–3046.

Large WG, Danabasoglu G, Doney SC, McWilliams JC. 1997. Sensitivity to surface forcing and boundary layer mixing in a global ocean model: annual-mean climatology. *Journal of Physical Oceanography* 27: 2418–2447.

Lukas R, Lindström EJ. 1991. The mixed layer of the western equatorial Pacific Ocean. *Journal of Geophysical Research* 96 (suppl.): 3343–3357.

Maes C, Picaut J, Belamari S. 2002. Salinity barrier layer and onset of El Niño in a Pacific coupled model. *Geophysical Research Letters* 29: article 2206.

Mignot J, de Boyer Montégut C, Lazar A, Cravatte S. 2007. Control of salinity on the mixed layer depth in the world ocean: 2. Tropical areas. *Journal of Geophysical Research* 112: C10010.

Monterey G, Levitus S. 1997. Seasonal variability of mixed layer depth for the world ocean. *NOAA Atlas NESDIS* No. 14. Washington DC: US Department of Commerce.

Pailler K, Bourlès B, Gouriou Y. 1999. The barrier layer in the western tropical Atlantic Ocean. *Journal of Geophysical Research* 26: 2069–2072.

Papa F, Durand F, Rossow WB, Rahman A, Bala SK. 2010. Satellite altimeter-derived monthly discharge of the Ganga-Brahmaputra River and its seasonal to interannual variations from 1993 to 2008. *Journal of Geophysical Research* 115: C12013.

Prasanna Kumar S, Nuncio M, Narvekar J, Kumar A, Sardesai S, de Souza SN et al. 2004. Are eddies nature's trigger to enhance biological productivity in the Bay of Bengal? *Geophysical Research Letters* 29: 88-1–88-4.

Rao RR, Sivakumar R. 2003. Seasonal variability of sea surface salinity and salt budget of the mixed layer of the north Indian Ocean. *Journal of Geophysical Research* 108: 3009.

Redelsperger J-L, Thorncroft CD, Diedhiou A, Lebel T, Parker DJ, Polcher J. 2006. African Monsoon Multidisciplinary Analysis: an international research project and field campaign. *Bulletin of the American Meteorological Society* 87: 1739–1746.

Shchepetkin AF, McWilliams J-C. 2005. The regional oceanic modeling system (ROMS): a split-explicit, free-surface, topography-following-coordinate oceanic model. *Ocean Modelling* 9: 347–404.

Shetye SR, Gouveia AD, Shankar D, Shenoi SSC, Vinayachandran P, Sundar N et al. 1996. Hydrography and circulation in the western bay of Bengal during the northeast monsoon. *Journal of Geophysical Research* 101: 14011–14025.

Spall MA, Weller RA, Furey PW. 2000. Modeling the three-dimensional upper ocean heat budget and subduction rate during the Subduction Experiment. *Journal of Geophysical Research* 105: 26151–26166.

Sprintall J, Tomczak M. 1992. Evidence of the barrier layer in the surface layer of the tropics. *Journal of Geophysical Research* 97: 7305–7316.

Tanguy Y, Arnault S, Lattes P. 2010. Isothermal, mixed, and barrier layers in the subtropical and tropical Atlantic Ocean during the ARAMIS experiment. *Deep-Sea Research I* 57: 501–517.

Varkey MJ, Murty VSN, Suryanarayana A. 1996. Physical oceanography of the Bay of Bengal and Andaman Sea. In: Ansell AD, Gibson RN, Barnes M (eds), *Oceanography and marine biology: an annual review*, vol. 34. London: Allen and Unwin. pp 1–70.

Appendix

Error estimates

Sensitivity tests allowed us to estimate the error on the barrier-layer (BL) computation. We first computed the barrier-layer thickness (BLT) for each month of the year, based on eight different criteria for the mixed layer depth (MLD) and the isothermal layer depth (ILD). We then evaluated the error as the standard deviation of the BL computed from each criterion from January to December. Note that the choice of the criterion was based on three parameters: $\Delta\sigma$ (density), ΔT (temperature), and the associated reference depth Z_o.